ACS APPLIED MATERIALS & INTERFACES

Research Article

www.acsami.org

Microscale Sensing of Oxygen via Encapsulated Porphyrin Nanofibers: Effect of Indicator and Polymer "Core" Permeability

Ruipeng Xue,[†] Chen Ge,[†] Kris Richardson,[‡] Andre Palmer,[‡] Mariano Viapiano,[§] and John J. Lannutti*[,†,∥]

[†]Department of Materials Science and Engineering, [‡]Department of Chemical and Biomolecular Engineering, and [∥]Department of Biomedical Engineering, The Ohio State University, Columbus, Ohio 43210, United States

[§]Department of Neurosurgery, Brigham and Women's Hospital, Harvard Medical School, Boston, Massachusetts 02115, United States

Supporting Information

ABSTRACT: Biomimetic polymer nanofibers integrate sensing capabilities creating utility across many biological and biomedical applications. We created fibers consisting of either a poly(ether sulfone) (PES) or a polysulfone (PSU) core coated by a biocompatible polycaprolactone (PCL) shell to facilitate cell attachment. Oxygen sensitive luminescent probes Pt(II) *meso*-tetra(pentafluorophenyl)porphine (PtTFPP) or Pd(II) *meso*-tetra(pentafluorophenyl)porphine (PdTFPP), were incorporated in the core via single-step coaxial electrospinning providing superior sensitivity, high brightness, linear response, and excellent stability. Both PES−PCL and PSU−PCL fibers provide more uniform probe distribution than polydimethylsiloxane (PDMS). PSU-based sensing fibers possessed optimum sensitivity due to their relatively higher oxygen permeability. During exposure to 100% nitrogen and 100% oxygen, PES−PCL fiber displayed an I_0/I_{100} value of 6.7; PSU−PCL exhibited a value of 8.9 with PtTFPP as the indicator. In contrast, PdTFPP-containing fibers possess higher sensitivity due to the long porphyrin lifetime. The corresponding I_0/I_{100} values were 80.6 and 106.7 for the PES−PCL and PSU−PCL matrices, respectively. The response and recovery times were 0.24/0.39 s for PES−PCL and 0.38/0.83 s for PSU−PCL which are 0.12 and 0.11 s faster, respectively, than the Pt-based porphyrin in the same matrices. Paradoxically, lower oxygen permeabilities make these polymers better suited to measuring higher (i. e., ∼20%) oxygen contents than PDMS. Individual fiber sensing was studied by fluorescence spectrometry and at a sub-micrometer scale by total internal reflection fluorescence (TIRF). Specific polymer blends relate polymer composition to the resulting sensor properties. All compositions displayed linear Stern−Volmer plots; sensitivity could be tailored by matrix or the sensing probe selection.

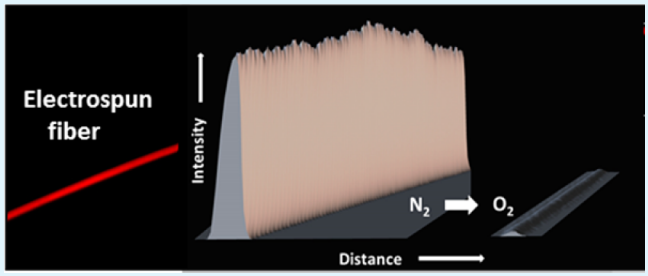

KEYWORDS: *hypoxia, oxygen sensor, electrospinning, luminescence, permeability, polyacrylonitrile*

INTRODUCTION

Oxygen is utilized by mammalian cells to enable energy production, a process fundamental to life, and in cell signaling and numerous enzymatic reactions critical to cell and tissue function.[1] Thus, measurement of molecular O_2 in biological systems (especially on a microscale) is of fundamental importance to understand the role of oxygen in cell biology, cancer research, and biomedicine.[2−4] Conventional Clark type electrodes consume oxygen during measurement and are difficult to miniaturize.[5] In contrast, optical oxygen sensors based on luminescence quenching have been developed and applied across many biological systems.[6] Oxygen probes are incorporated in a matrix and changes in luminescence intensity or lifetime used to quantify oxygen levels. These sensors do not consume oxygen, are noninvasive are easily miniaturized, and enable imaging of oxygen levels. Existing sensors exhibit significantly different levels of sensitivity and other properties and take a variety of forms depending on the specific application, from nanosized particles for intracellular measurements to the thin films found in microfluidic devices.[7−9] Among them, thin-film-based sensors are the most widely studied form. Oxygen probes are either directly incorporated in these films or doped into particles which are then mixed with the film matrix. The sensitivity of such films is directly related to both the probe performance and the permeability of the film. A large selection of polymers has been investigated as matrix materials; most are highly gas permeable, e.g., polydimethylsiloxane, ethyl cellulose, and poly(2-hydroxyethyl methacrylate).[10−12] Although such thin films are relatively easy to prepare, they are not suitable for biological applications on both the small scale (as the biofilm interface is purely planar) and neither can they report the kind of three-dimensional information required by current and future tissue engineering operations.

Recently, nanosized fibers fabricated by electrospinning have been shown to be suited to oxygen-sensing applications.[13,14]

Received: January 22, 2015
Accepted: April 8, 2015
Published: April 8, 2015

DOI: 10.1021/acsami.5b00403
ACS Appl. Mater. Interfaces 2015, 7, 8606−8614

Such nanofiber-based sensors show linear response to both gaseous and dissolved oxygen while maintaining biocompatibility and good cell adhesion due to a 3D structure that mimics the extracellular matrix (ECM). Such nanofibers possess small diameters and high surface-to-volume ratios allowing for rapid sensing in dynamically changing biological or industrial environments. Like other luminescence optical sensors, sensitivity, linearity, stability, and response time are dependent on both the luminescent sensing probe and the host material as well as their interactions. Probe/materials selection, matrix composition, sensor format, and the desired sensor performance must be well controlled or tailored for specific applications on a case-by-case basis.

The most widely studied oxygen-sensitive probes are transition metal−ligand complexes or metalloporphyrins. Among them, platinum(II) *meso*-tetra(pentafluorophenyl)-porphine (PtTFPP) and palladium(II) *meso*-tetra-(pentafluorophenyl)porphine (PdTFPP) have attracted considerable interest due to their sensitivity to oxygen and excellent brightness and stability.[15] PtTFPP, in particular, possesses excellent photostability in matrix materials under continuous excitation.[16] In contrast, PdTFPP has higher sensitivity than its platinum counterpart due to its inherently longer excited state lifetime (1.65 ms for PdTFPP versus 60 μs for PtTFPP).[17,18] Interestingly, the "oversensitivity" of PdTFPP is thought to limit more general applications of this sensing moiety.

In terms of the polymer serving as a host for these porphyrins, considerable effort has been directed toward matrix polymers having excellent oxygen permeability, typically silicones. However, in many of these cases the porphyrin may have limited solubility or long-term compatibility with the polymer matrix. Low solubility can lead to probe molecule segregation resulting in nonlinear Stern−Volmer curves[19] or, in some cases, visibly heterogeneous probe distribution[20] making quantitative oxygen distribution imaging difficult. Probe molecule aggregation and continued migration can also adversely affect performance stability.[15] For these reasons, polymer matrices providing excellent probe solubility are preferred.

Polymers having good solubility along with lower gas permeability can also have attractive overall properties such as better optical clarity, superior mechanical properties, and high chemical/thermal stability. A strategy that may allow one to take full advantage of these properties while still maintaining the desired sensitivity involves compensation for low oxygen permeability by careful selection of long-lived luminescent oxygen probes. To test this hypothesis, we selected two less gas permeable polymers, poly(ether sulfone) (PES) and polysulfone (PSU), as matrices for optical oxygen sensing due to their optical clarity and mechanical strength. The two polymers are structurally similar but possess contrasting levels of oxygen permeability that are only 0.04−0.22%[21] that of polydimethylsiloxane (PDMS). The matrix materials were fabricated as nanosized fibers for potential biological applications by electrospinning. Core−shell nanofibers in which probe-free polycaprolactone (PCL) forms the "shell" provide improved biocompatibility and overcome production and handling issues associated with fibers formed only from polymers having high elastic moduli (i. e., PES and PSU). Blends of these two polymers were also studied to establish the relationship between matrix composition and sensing properties. Two sensing probes—PtTFPP and PdTFPP—having different levels of oxygen sensitivity were incorporated separately into these nanofiber matrices. In all cases, the oxygen-sensitive fibers show higher brightness, high levels of uniform porphyrin incorporation, and stable luminescence under continuous illumination. To provide a more exhaustive evaluation, sensing properties were evaluated at both the macroscopic (fiber mats) and the microscopic (individual fiber) levels. In addition, we compared the behavior of the relatively oxygen-impermeable matrix, polyacrylonitrile (PAN), as a "negative control."

In this work, we investigated a series of nanofiber-based optical sensors that possess superior stability, high sensitivity, and linear response and by using these sensors we successfully obtained oxygen information from single-fiber scale. We established that in nanofiber form even low gas permeability polymer matrices can be successfully used as fast oxygen sensors providing both stable performance and the necessary sensitivity. Sensor properties could be finely tuned by the appropriate selection of matrix and sensing probe molecule. A suitable combination of relatively low-cost polymers and sensitive molecular oxygen probes in electrospun form provides a useful tool for monitoring oxygen levels in biological applications.

EXPERIMENTAL SECTION

Materials. PtTFPP and PdTFPP were obtained from Frontier Scientific Inc. (Logan, UT, USA). Dichloromethane (DCM) was acquired from Sigma-Aldrich (St. Louis, MO, USA), and 1,1,1,3,3,3-hexafluoro-2-propanol (HFP) from Oakwood Products Inc. (West Columbia, SC, USA) was used without further purification. Polysulfone (PSU, Mn ∼ 16,000) and polycaprolactone (PCL, Mn ∼ 70,000−90,000) were both purchased from Sigma-Aldrich. Poly(ether sulfone) (PES, Mn ∼ 55,000) was purchased from Goodfellow Corp. (Huntingdon, England), and polyacrylonitrile (PAN, Mw ∼ 150,000) was purchased from Sigma-Aldrich.

Preparation of Core−Shell Nanofibers. Initially, 5 mg of each probe (either PtTFPP or PdTFPP) was dissolved in 1:1 DCM/HFP. Afterward, 0.5 g of PES or PSU needed to form the fiber "core" was added followed by stirring to dissolve the polymer (15 wt %) forming a visually uniform, red solution. A PCL solution was prepared by dissolving 0.5 g of PCL in 9.5 g of HFP to form a 5 wt % solution. Solutions were loaded in 5 mL syringes and controlled by two syringe pumps with flow rates of 2:4 mL/h (core:shell). A homemade needle was used to feed the solution in a coaxial manner, and core−shell fibers were electrospun. The PCL "shell" did not contain any probe. As a result, the final core−shell fibers contain approximately 6 mg of porphyrin/(g of fibers). The applied voltage between the needle and the collector (20 cm in distance) was 25 kV. Fibers were collected on aluminum foil to form fiber mats (100 μm in thickness) or glass coverslips to achieve single-layer deposition for microscopy imaging. Polyacrylonitrile nanofibers containing palladium porphyrin were prepared following procedures described in the literature.[22] All fiber samples were placed under vacuum overnight to fully remove any residual solvent[23] and were stored in darkness prior to testing.

Measurements. Fiber diameter and morphology were examined using scanning electron microscopy (SEM, XL30 ESEM, FEI Co., Hillsboro, OR, USA). The luminescence properties of the fiber mats were studied using a JAZ fluorescence spectrometer (Ocean Optics Inc., Dunedin, FL, USA). Fiber mat samples were placed in glass cuvettes, and a spectrometer probe was directed toward the sample both to excite the fiber via 470 nm light and to collect the resulting emission. Specific gaseous oxygen concentrations were created by flowing specific oxygen/nitrogen mixtures through a gas flow meter (Omega Engineering, Stamford, CT, USA) connected to the cuvette containing the fiber mats. When the samples were immersed in water to enable calibration of dissolved oxygen contents, oxygen composition was controlled by bubbling the same specific gas mixtures in water until equilibrium was achieved. An oxygen meter (HQ40d,

DOI: 10.1021/acsami.5b00403
ACS Appl. Mater. Interfaces 2015, 7, 8606−8614

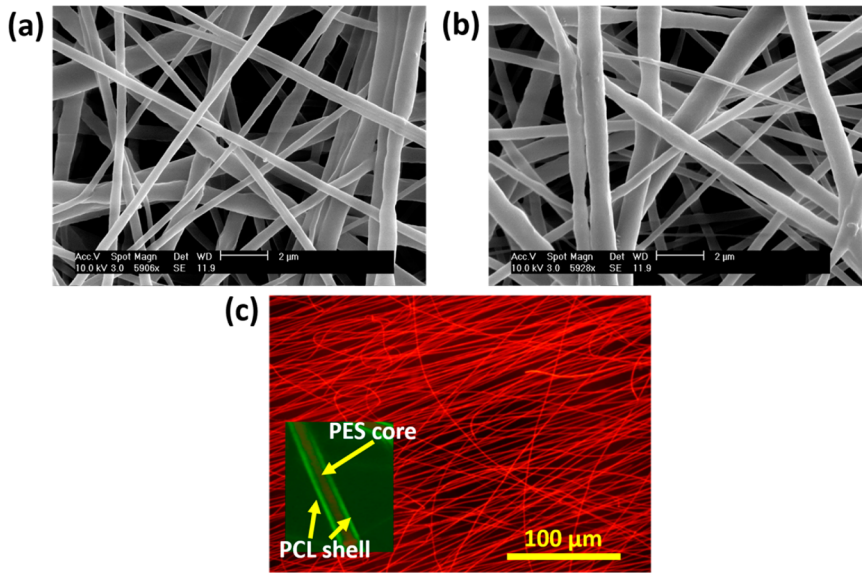

Figure 1. SEM images of (a) PES−PCL and (b) PSU−PCL fibers containing PtTFPP oxygen probe; (c) fluorescence image of PES(PtTFPP)−PCL fibers with a merged inset showing the core−shell structure.

Hach Co., Loveland, CO, USA) was used to confirm that the desired oxygen levels had been reached.

Spectral emission was monitored to create a calibration allowing determination of unknown oxygen levels. The calibration for both the gaseous phase and dissolved oxygen followed the Stern−Volmer equation[24]

$$I_0/I = 1 + K_{SV}[O_2] \quad (1)$$

where I_0 and I are the luminescence intensity in the absence and presence of oxygen, respectively, and $[O_2]$ is the corresponding oxygen concentration. K_{SV} is the Stern−Volmer coefficient.

Sensor reversibility was evaluated by continuously monitoring the emission peak as the environment was rapidly switched between oxygen and nitrogen. For comparison purposes, nitrogen or oxygen gas flow rate is maintained at the same levels for all tests of reversibility. The response/recovery times defined as the time required for 95% of the total intensity change to occur were calculated based on the reversibility data. Similarly, tests of photostability were conducted by continuous excitation and monitoring of the emission peak for extended times (typically about 90 m). Probe leaching was investigated by immersing samples in water at 37 °C for 1 week; sample emission following standard levels of excitation was measured every 24 h.

Image Analysis. For microscopy analysis, a thin layer of core−shell fibers was electrospun onto 30 mm diameter circular coverslips and assembled in an interchangeable coverslip dish (Bioptechs Inc., Butler, PA, USA) providing environmental control. Fluorescence images of the fibers were taken using total internal reflection fluorescence (TIRF, TiE Nikon Inc. Melville, NY, USA) microscopy under different oxygen contents following excitation by a 561 nm laser. The intensity profile of individual fibers was analyzed using NIH ImageJ with the ND Viewer Plugin. Stained cells cultured on the fibers were imaged by exciting them with a 488 nm laser.

Statistical Analysis. Analysis of variance (ANOVA) and Tukey−Kramer HSD tests were carried out for the PES/PSU blend results using the statistical analysis software JMP Pro (10.10.2). p-values < 0.05 were considered statistically significant.

Cell Culture. Glioblastoma cell lines U251MG cells were cultured in Dulbecco's modified Eagle's medium (DMEM) containing 4.5 g/L glucose and 10% (v/v) fetal bovine serum. A 50 UI/mL amount of penicillin and 50 μg/mL streptomycin were added to the culture media to prevent bacterial growth. When cells reached 80% confluency in the culture dish, they were dissociated and seeded at an average density of 10,000 cells/well in the 8-well self-adhesive μ-Slide (ibidi, Planegg, Germany) having a core−shell fiber-covered polystyrene bottom. Cells were cultured on the fibers for about 12 h to allow attachment and then imaged on an epifluorescence microscope (Eclipse, Nikon).

RESULTS AND DISCUSSION

Preparation and Characterization of PES−/PSU−PCL Core−Shell Nanofibers. PES/PSU core, PCL shell nanofibers fabricated by coaxial electrospinning contain the fluorescent probes only within the core. SEM images (Figure 1a,b) show that the morphology of these core−shell fibers containing the PtTFPP porphyrins in the core is typical of that of many electrospun fibers.[25] The average fiber diameters are 615 ± 221 nm for PES−PCL and 732 ± 265 nm for PSU−PCL, respectively. The highly porous structure of the fiber mats allows rapid gas exchange enabling fast sensor response. The biocompatibility provided by the PCL shell has been demonstrated in previous work.[13] Biocompatible PCL facilitates cell adhesion while having no measurable effects on sensing performance. If either PES or PSU was electrospun without the PCL shell, the resulting deposition efficiency was low and the fibers themselves formed brittle, cotton-like mats. The addition of the PCL shell drives the behavior of the falling fiber such that these core−shell fibers electrospin and behave in a manner mechanically similar to pure PCL during and after the process. Subsequent applications can require thin fiber layers having either random or aligned orientations deposited on a variety of surfaces. Rather than the loose adhesion characteristic of pure PES or PSU nanofibers, the addition of a PCL shell greatly improves the ability of the core−shell fibers to adhere to even insulating surfaces such as glass.

The successful incorporation of the probe in the fibers is validated by the associated fluorescence (Figure 1c). The optimized probe loading concentration in the fiber core was found to be 1 wt % which provided a strong emission without the probe aggregation expected from a similarly high loading in PDMS. These fibers emit a bright, uniform red fluorescence upon excitation in oxygen-free environments. The observed brightness is significantly higher compared to our previous studies of PCL or PDMS fibers under identical excitation.[13,26] This strong signal is a function of both the luminescent

DOI: 10.1021/acsami.5b00403
ACS Appl. Mater. Interfaces 2015, 7, 8606−8614

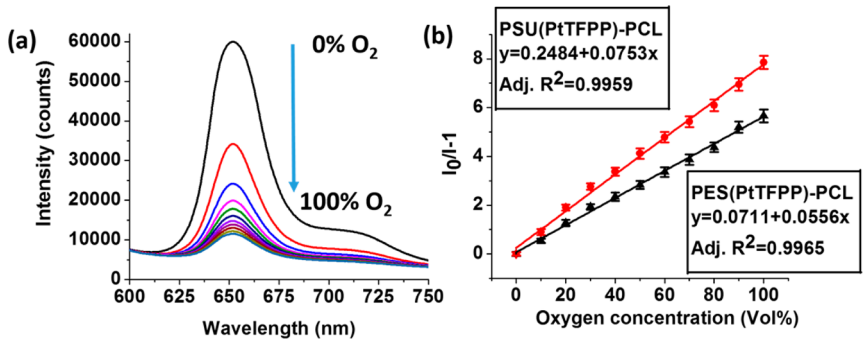

Figure 2. (a) Emission spectra and responses to gaseous oxygen of PSU(PtTFPP)−PCL fibers; (b) Stern−Volmer plots of PES(PtTFPP)−PCL and PSU(PtTFPP)−PCL fibers for gaseous oxygen.

properties of the probe and the excellent probe−matrix compatibility. Probe brightness is the product of molar absorption coefficient and quantum yield and is important for any sensor application at a local (individual fiber) scale. High brightness also allows the use of lower probe concentrations if desired. Finally, these fibers did not exhibit noticeable photobleaching even following continuous excitation over a period of 10 min. As the merged image of fluorescence and bright field shows (inset of Figure 1c), the core−shell structure was successfully produced and a defined boundary between the probe-containing PES/PSU core and the probe-free PCL shell is visible. This unique structure avoids contact between cells and a potentially toxic fluorescent dye while allowing gas molecules to easily diffuse through the relatively thin PCL shell.

Sensing Performance of PtTFPP-Doped PES−PCL and PSU−PCL Fibers. Fiber mats containing PtTFPP showed sharp emissions centered at 654 nm for PES and 652 nm for PSU when excited by a blue LED. The large Stokes shift between absorption and phosphorescence creates less interference from the excitation light creating clear spectral signal separation. The peaks are efficiently quenched by gradually increased amounts of gaseous oxygen as shown in Figure 2a for PSU−PCL. This dynamic quenching involves collisions between the triplet ground state molecular oxygen and the excited triplet electronic state of the probe molecule, often resulting in the formation of singlet oxygen.[27] Exposed to 0 and 100% oxygen, PES(Pt)−PCL fiber displays an I_0/I_{100} value of 6.7 while PSU(PtTFPP)−PCL exhibits a higher value of 8.9. This difference is likely the result of differences in gas permeability between the two core polymers. The two polymers share similar backbone structures, but PSU has a substantially higher oxygen permeability coefficient (91 cm^3 mm/(m^2 day atm)) than PES (14.6 cm^3 mm/(m^2 day atm)).[21] When the same luminescent probe is involved, the oxygen permeability of the polymer matrix partly determines the amount of oxygen that reaches the probe molecules and regulates ultimate sensitivity. In fiber form, both of these compositions are better suited to applications involving higher O_2 levels (e.g., in air) than PDMS as they exhibit more intense emission from the core. Under such circumstances it becomes easier to detect, separate, and quantify luminescent performance especially in imaging-based applications.

Emission values at different oxygen concentrations could be converted to a linear response curve using the Stern−Volmer equation. The Stern−Volmer curves for PES(PtTFPP)−PCL and PSU(PtTFPP)−PCL are plotted in Figure 2b. In accordance with its higher oxygen diffusivity, PSU displays higher sensitivity as the SV plot has a larger slope. The error bars of the Stern−Volmer plots originated from multiple measurements of samples from different batches and the intensity fluctuation of the emission peaks. Such small signal fluctuations are a limitation of the intensity-based method, and this problem can be addressed by using either lifetime-based measurements or by adding a reference emitter.[6,18,27]

Both matrices provide excellent (adjusted $R^2 > 0.99$) linear response and satisfactory sensitivity. A linear Stern−Volmer curve is critical in providing accurate calibration and straightforward data analysis. Linearity is an indication of good probe−matrix compatibility and uniform probe distribution. In contrast, a downward curvature would be observed if the probe molecules existed in a variety of configurations or environments.[6] The associated theory assumes that the probe molecules are distributed in at least two sites creating populations that express different quenching abilities.[28] A multisite model is then required to mathematically describe these downward response behaviors and convert them to a linear Stern−Volmer curve.

While the fibers were continuously excited, the emission peak intensity for each probe molecule was monitored and plotted under conditions alternating between 100% oxygen and 100% nitrogen. Responses to both gases were fully reversible, and the signal remained constant after either response or recovery. (Figure 3) The response time (t_{95}) and recovery time can be

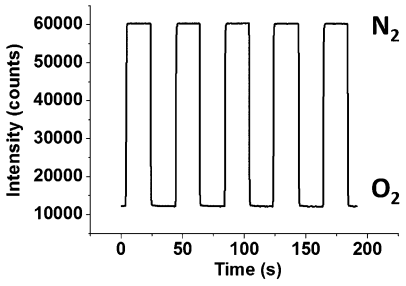

Figure 3. Reversibility of PSU(PtTFPP)−PCL fibers under alternating oxygen and nitrogen gases.

calculated from these reversibility plots. For PSU(PtTFPP)−PCL, it took 0.49 ± 0.06 s to respond (nitrogen to oxygen) and 1.12 ± 0.03 s to fully recover (oxygen to nitrogen). Note that this response time also includes time needed to fully flush the environment in the 10 mL cuvette. Therefore, the actual response should be faster than that determined here. The response and recovery times for PES(PtTFPP)−PCL fibers were generally faster than PSU likely due to PES' lower

DOI: 10.1021/acsami.5b00403
ACS Appl. Mater. Interfaces 2015, 7, 8606−8614

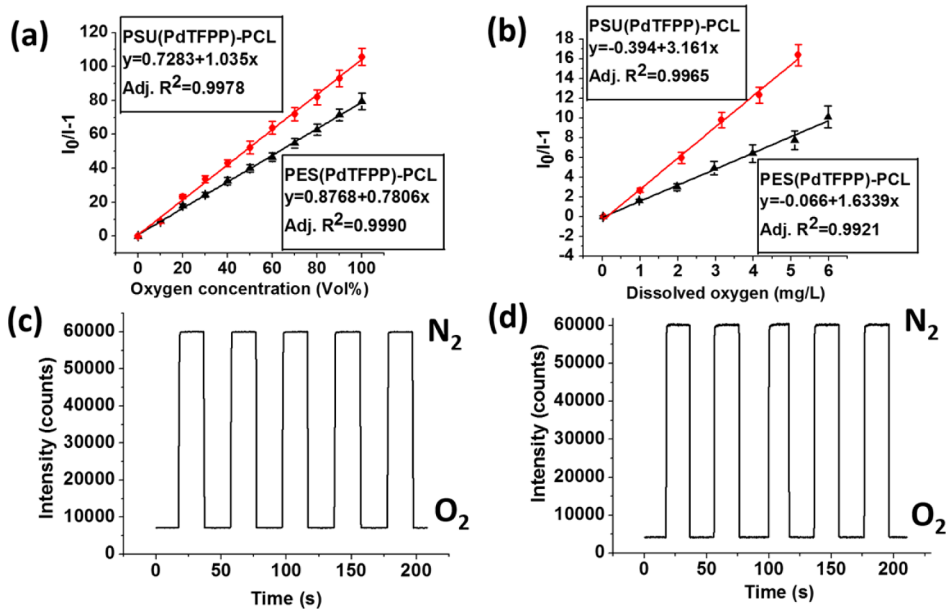

Figure 4. (a) Stern–Volmer plots of PES(PdTFPP)–PCL and PSU(PdTFPP)–PCL in different gaseous oxygen concentrations; (b) PES(PdTFPP)–PCL and PSU(PdTFPP)–PCL for dissolved oxygen in 37 °C water; reversibility of (c) PES(PdTFPP)–PCL and (d) PSU(PdTFPP)–PCL in oxygen/nitrogen.

permeability. We also investigated the effects of fiber diameter on response/recovery time. By increasing the PES polymer solution concentration to 15 wt % and the flow rate of the PES solution to 5 mL/h during electrospinning, the as-fabricated fibers were increased in diameter from 465 to 811 nm. As a result, the response time also increased from 0.36 ± 0.06 to 0.80 ± 0.16 s. Similarly, the recovery time was 0.66 ± 0.05 s for smaller diameter PES–PCL fibers and 2.22 ± 0.003 s for the same composition having a larger diameter. It should be noted, however, that the sensitivities of fibers with different diameters are almost identical. Smaller fiber diameters reduce diffusional limitations and decrease response time but do not significantly affect sensitivity controlled primarily by oxygen permeability.

Sensing Performance of PdTFPP-Doped PES–PCL and PSU–PCL Fibers. Compared to most commonly used polymer matrix materials, the gas permeabilities of PES and PSU are lower and therefore the PtTFPP in these fibers does not show as high a sensitivity as many other sensors.[29] To take full advantage of the greater compatibility that PES and PSU provide, a similar porphyrin, PdTFPP, having a much longer excited state lifetime (1.65 ms versus 60 μs) was incorporated into these same core–shell fibers. The fibers containing the palladium porphyrin are essentially the same in terms of electrospinnability and morphology. However, the spectral responses of PES(PdTFPP)–PCL and PSU(PdTFPP)–PCL to oxygen are very different from otherwise identical core–shell fibers containing PtTFPP. The emission peaks are centered at 674 nm for the PES core fiber and 673 nm for the PSU core fibers. Sensitivities are significantly improved for both cases such that ~20% oxygen greatly reduced the emission peak. The corresponding I_0/I_{100} values are 80.6 and 106.7 for PES and PSU, respectively. As expected, the corresponding Stern–Volmer plots have much larger slopes while still maintaining the excellent linearity (Figure 4a), characteristic of electrospun fiber sensors.[13] The adjusted R^2 values for the linear fit to the PES(PdTFPP)–PCL and PSU(PdTFPP)–PCL data are 0.9990 and 0.9978, respectively. The longer lifetime of palladium porphyrins versus their platinum counterparts is believed to be due to the increased spin–orbit coupling associated with the heavier metal.[30] PdTFPP is extremely sensitive to oxygen and can be used in sensors designed to detect the presence of even trace amounts of oxygen.[31] Oxygen can efficiently quench the emission of the PdTFPP within highly oxygen-permeable polymers, and this could be a problem if sensing in relatively high oxygen environments such as air is desired. PES or PSU appeared to overcome this limitation by allowing *less* oxygen diffusion while allowing levels of total diffused oxygen to remain proportional to these found in the surrounding environment.

To test using a more biologically relevant condition, fibers containing PdTFPP were calibrated in 37 °C water to report levels of dissolved oxygen (DO). The Stern–Volmer plots (Figure 4b) were created for water containing up to ~6 mg/L DO. Similar to the gaseous oxygen measurements, highly linear Stern–Volmer plots were obtained in which the PSU matrix again exhibited larger slopes than did PES. The slopes of linear fit curves are 1.63 and 3.16 $(mg/L)^{-1}$ for the PES(PdTFPP)–PCL and PSU(PdTFPP)––CL fibers, respectively. High sensitivity allows easy quantification of oxygen variation based on the image analysis of these fibers when applied to cell culture. The high thermal, biological and mechanical stability of the PES or PSU core assures proper performance of the fibers under challenging biological conditions. The PCL protective shell provides a biocompatible external surface while the inner core prevents water diffusion and other ionic interference that could adversely affect sensing performance.

Part c and d of Figure 4 show the emission intensity changes as the environment was repeatedly switched between oxygen and nitrogen. The fibers display an even faster response to or recovery from applied oxygen contents than fibers containing platinum porphyrins. The calculated response and recovery times are 0.24 ± 0.02/0.39 ± 0.03 s for PES–PCL and 0.38 ± 0.03/0.83 ± 0.04 s for PSU–PCL. The response times are 0.12 and 0.11 s faster for PdTFPP in PES and PSU, respectively, versus the platinum-containing probe in the same matrices. The higher oxygen sensitivity, small fiber diameters, and large

DOI: 10.1021/acsami.5b00403
ACS Appl. Mater. Interfaces 2015, 7, 8606–8614

surface-to-volume ratio allow rapid gas exchange and a fast response allowing real-time monitoring of oxygen change in biological processes.[10]

Blends of PES and PSU as the Core Containing PdTFPP. Although PdTFPP showed good sensing properties when dissolved in the core of both PES−PCL and PSU−PCL fibers, the two sensors are distinct in terms of their sensitivity to both gaseous and dissolved oxygen. In specific applications, it will be useful to have the ability to easily "tune" the sensor to achieve the desired sensitivity. To investigate this possibility, blends of PES and PSU with PdTFPP were electrospun to create the porphyrin-containing core of the core−shell fiber to explore the possibility of tailoring the sensitivity by varying the blend composition. Weight ratios (PSU/PES) of 0/100, 20/80, 50/50, 80/20, and 100/0 were studied and all were successfully electrospun as the core in core−PCL shell fibers. Stern−Volmer plots for each composition continued to exhibit good linearity ($R^2 > 0.9950$). However, the composition of the blend evidently affects net sensitivity. If the slope of the SV plot represents sensitivity, the plot of slope versus composition is found in Figure 5. The addition of 20 wt % PES into PSU

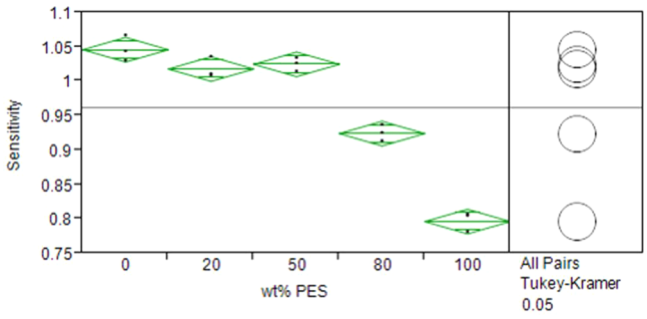

Figure 5. Change in sensitivity as a function of composition and Tukey−Kramer HSD test for sensitivity and PES/PSU polymer composition.

slightly decreased the slope from 1.05 $(\%)^{-1}$ to 1.01 $(\%)^{-1}$, but at 50/50 composition the slope recovered somewhat to 1.03 $(\%)^{-1}$. The sensitivity then decreased significantly with increasing amounts of PES (from 50 to 100 wt %). Statistical test of ANOVA shows that sensitivity is significantly dependent on polymer composition. In particular, the Tukey−Kramer HSD test shows that fibers made up of 0, 20, and 50% PES are not significantly different in terms of sensitivity but differences between these and the other compositions are statistically significant likely due to the corresponding oxygen permeability difference. Even though the sensitivity was adjustable, excellent linearity was retained by all of the compositions. Therefore, sensitivity can be controlled by systematic variation of the weight ratio of the two polymers and the desired level tailored for specific applications obtained. The sensitivity vs weight percent PES plot reveals that sensitivity is a synergistic effect rather than an average dictated by composition.

Polyacrylonitrile Fibers Containing PdTFPP. Polyacrylonitrile (PAN) fibers were evaluated in this study as a "negative control" because it is widely considered to be highly oxygen impermeable and is often used as an oxygen barrier.[32] Interestingly, PAN electrospun fibers containing PdTFPP still show oxygen sensitivity although the response/recovery times were considerably slower. The PAN fiber showed an I_0/I value of 4.8 when cycled between nitrogen and oxygen. As already discussed, the long-lived excited state lifetime of PdTFPP is in milliseconds and is highly susceptible to dynamic quenching by environmental oxygen. Thus, even the trace amounts of oxygen that penetrate the small-diameter PAN fibers partially quench the phosphorescence emission and facilitate oxygen sensitivity. As shown in Figure 6, however, the shape of the cyclic exposure

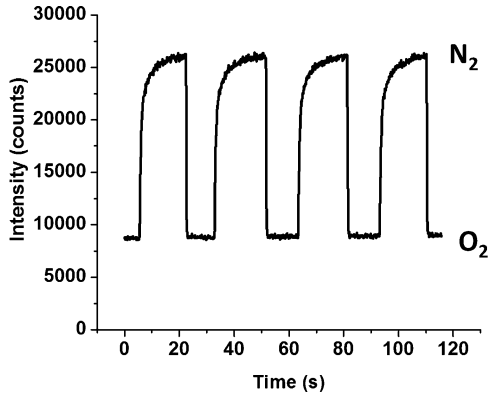

Figure 6. Response and recovery of PAN(PdTFPP) fibers.

plot is quite different from the other matrix compositions (Figure 4c,d). While the response time is 0.92 ± 0.06 s, the recovery time is much longer: 8.3 ± 0.31 s. The electrospun PAN fibers possess a high surface area comparable to that of PES−PCL or PSU−PCL fibers; thus it is unlikely that the gas exchange is limited by surface absorption or desorption. The slower response to oxygen compared to PES−PCL or PSU−PCL fibers is probably due to the intrinsically low oxygen permeability of PAN. The recovery time of PAN is 9 times longer than its response time due to the fact nitrogen diffusion is even slower than oxygen diffusion in this matrix.[21] This also holds true for the previously discussed PES−PCL or PSU−PCL fibers as these recovery times are always longer than the response times. In the PAN fiber case, however, the differences in nitrogen and oxygen permeability are exaggerated by the excellent gas barrier properties of PAN.

Image Analysis and Individual Fiber Sensing. Biological applications often dictate that oxygen be reported on a local or cellular level. Thus, the ability of these oxygen sensing nanofibers to operate at small scales is of great interest. Fibers deposited on glass coverslips were imaged by TIRF microscopy under controlled environments. Parts a and b of Figure 7 show the appearance of the same PES(PdTFPP)−PCL fiber under different compositions of atmospheric oxygen (0 and 100%). While the fiber exhibits very strong emission in an oxygen-free environment, it is barely visible at $[O_2]$ well above 20%. Image analysis of the single fiber should—in theory—reveal the same quantitative oxygen sensitivity captured by SV plots derived macroscopically from the fiber mats. For the single fiber shown in the images, the intensity profile versus distance along the fiber was recorded (Figure 7c is the source of Figure 7a) and the average intensity corresponding to different oxygen concentrations determined. Figure 7d provides the corresponding averaged Stern−Volmer plot for this single PES(PdTFPP)−PCL fiber. The Stern−Volmer curve maintains the same 0.81 $(\%)^{-1}$ slope and linearity (adjusted R^2= 0.99227) over the full range of oxygen exposures. It should be noted that even though the fiber appeared uniform in the image, the surface plot in Figure 7c exhibits small variations in intensity. This variation may be due to minor changes in fiber diameter,

DOI: 10.1021/acsami.5b00403
ACS Appl. Mater. Interfaces 2015, 7, 8606−8614

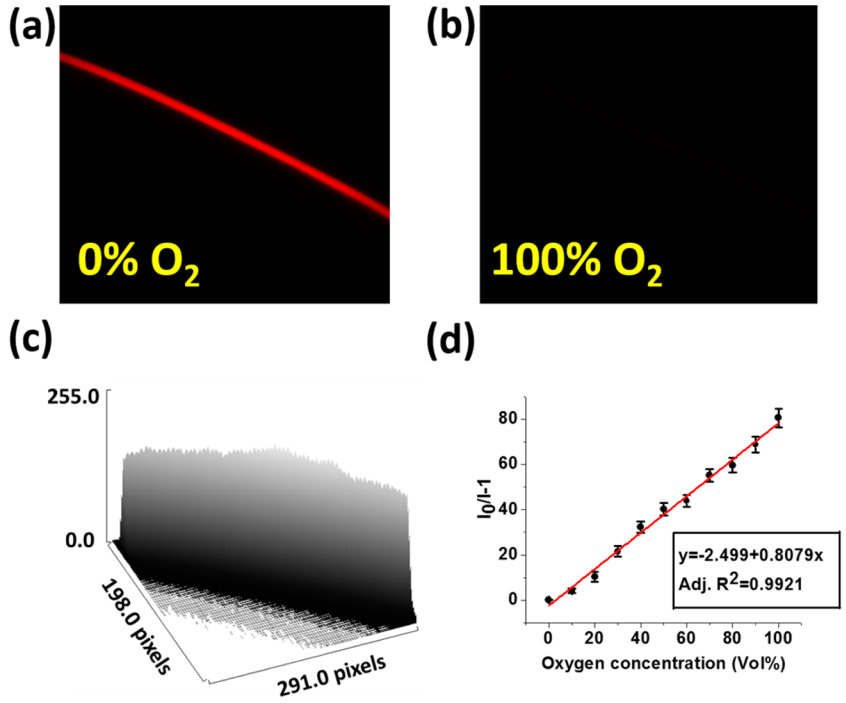

Figure 7. Single PES(PdTFPP)−PCL fiber under (a) 0% and (b) 100% oxygen; (c) intensity surface plot of image a; (d) the associated Stern−Volmer plot derived from an average of the peaks in c.

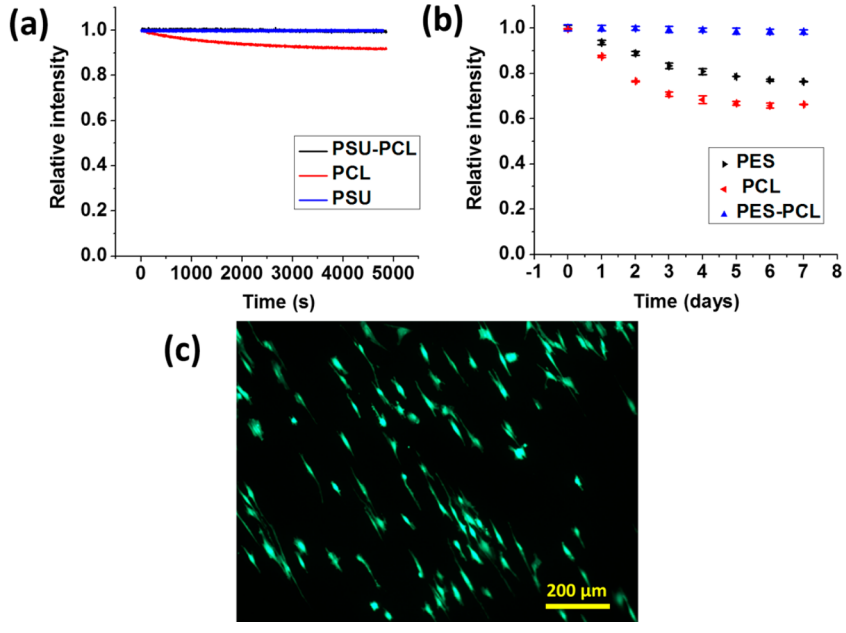

Figure 8. (a) Photostability tests of PSU−PCL, PSU, and PCL fibers containing PdTFPP under continuous excitation; (b) comparison of noncore−shell fibers with core−shell fiber emission during extended exposure to water at 37 °C; (c) U251 cells cultured on aligned PSU(PdTFPP)−PCL fibers under normoxia.

uneven luminescent probe distribution, or nonuniform excitation.

The ideal matrix material serves as solvent for the luminescent probe, provides appropriate mechanical support, improves selectivity by preventing penetration of interfering species such as iodides, and, most importantly, correctly adjusts the quenching behavior of the sensor.[33] Polymeric films are straightforward and inexpensive to make using spin or dip coating and have been used extensively to create oxygen sensors. A variety of film-based oxygen sensors have been studied including PDMS, ethyl cellulose, poly(methyl methacrylate), polystyrene, and hydrogel, etc.[6] For example, polystyrene microwells have been produced by embossing PDMS stamps.[34] In addition, biocompatible core−shell oxygen sensing particles have been produced to attempt to create intracellular imaging of oxygen content.[35] However, to apply extracellular sensors in commonly created biological environments (such as tissue engineering operations), sensor forms other than thin films or nanoparticles are required to provide faster response times and three-dimensional oxygen distribu-

DOI: 10.1021/acsami.5b00403
ACS Appl. Mater. Interfaces 2015, 7, 8606−8614

tions and to provide a more biomimetic environment for living cells. On contrast, nanofiber sensor forms are particularly suitable in extracellular applications due to the fact that they are biocompatible and biomimetic and can be easily incorporated into cell culture.

Sensor Stability. A general concern for luminophores is that slow photobleaching has been observed after repeated sampling or long-term continuous excitation. Reactive singlet oxygen, a product of the oxygen quenching process, is generally believed to be responsible for photobleaching by photo-oxidation of the probe.[36,37] However, the photodegradation rate observed for core−shell fibers in this study is quite low. Figure 8a is the intensity of the emission peak as a function of time (up to 5000 s) under continuous LED excitation as monitored by a spectrometer for PSU−PCL and PSU and PCL fibers containing PdTFPP. The test suggests that the probes in PSU and PSU−PCL core−shell fibers have excellent photostability and could be used continuously with only negligible drift. The fluorine substituents of these porphyrin rings improve photodegradation resistance by increasing the redox potentials and the molecular electron density.[6] Excellent probe compatibility enables uniform probe molecule distribution, and the speed of the electrostatic forming process avoids the aggregation that often leads to self-quenching. Solids ^{19}F NMR (Supporting Information) show that the chemical environment of the porphyrin is the same for both PES (Supporting Information Figure S1) and PSU (Supporting Information Figure S2) in which the ^{19}F peaks display minimal splitting. PCL (Supporting Information Figure S3) as a matrix, in contrast, creates poor mixing[26] and multiple chemical environments for the fluorine. As a result of this excellent dispersion, PSU−/PES−PCL fibers all express strong luminescence without noticeable signal degradation even after exposure to continuous excitation. The fibers remained stable after 6 months storage at room temperature and showed fully reproducible results.

The fibers were soaked in 37 °C water, and their emission was monitored to assess probe leaching, another common problem that can prevent accurate sensing. A comparison of PES, PCL, and PES−PCL leaching tests for extended times (7 days) was conducted; the results are shown in Figure 8b. The core−shell structure significantly eliminates probe molecule leaching compared to either single-phase PES or PCL fibers from which probe molecule leaching can occur. This is the result of both excellent solubility within the core matrix and the protection provided by the presence of a PCL shell.

Figure 8c demonstrates that U251 cells could be cultured and attached to the aligned PSU(PdTFPP)−PCL fibers. Cells show typical behavior on aligned electrospun fibers in which they actively follow the direction of fiber alignment.[38] The PCL shell serves as a barrier against the diffusion of water and other ionic species to effectively maintain the sensing properties of the fibers in complex biological environments. Prevention of probe leaching not only assures accurate sensing results but also reduces any potential cytoxicity with the surrounding cells.

CONCLUSIONS

Core−shell electrospun polymer fibers provide an appropriate format for high brightness oxygen sensors. Combined use of low gas permeability polymers and probes having long luminescence lifetimes creates sensors having attractive properties. Small fiber diameters and large surface-to-volume ratios allow rapid gas exchange and a fast response appropriate to real-time monitoring of oxygen changes in biological processes. The sensing properties of the poly(ether sulfone)- and polysulfone-based nanofiber sensors are greatly different due to contrasting levels of oxygen permeability. Sensitivity can be controlled by systematic variation of the weight ratio of the two polymers and levels tailored to specific applications obtained.

ASSOCIATED CONTENT

Supporting Information

Figures showing 300 MHz fluorine-19 MAS NMR spectra of electrospun PdTFPP-containing PCL−PES, PdTFPP-containing PCL−PSU, and PdTFPP-containing PCL−PCL core−shell fibers suggesting substantial differences in probe aggregation. This material is available free of charge via the Internet at http://pubs.acs.org.

AUTHOR INFORMATION

Corresponding Author

*E-mail: Lannutti.1@osu.edu.

Notes

The authors declare no competing financial interest.

ACKNOWLEDGMENTS

This work was partly supported by a research grant from the National Science Foundation under Grant Nos. CMMI-0928315 and EEC-0425626 and the Ohio State Institute for Materials Research (IMR). Any opinions, findings, and conclusions or recommendations expressed in this material are those of the authors and do not necessarily reflect the views of the National Science Foundation or the National Institutes of Health. We thank the University of Akron Department of Chemistry for providing access to their 300 MHz fluorine-19 MAS NMR spectrometer. We also gratefully thank Carlos Castro for graciously allowing access to his total internal reflectance fluorescence microscope.

REFERENCES

(1) Semenza, G. L. Life with Oxygen. *Science* **2007**, *318*, 62−64.
(2) Napp, J.; Behnke, T.; Fischer, L.; Wuerth, C.; Wottawa, M.; Katschinski, D. M.; Alves, F.; Resch-Genger, U.; Schaeferling, M. Targeted Luminescent Near-Infrared Polymer-Nanoprobes for in Vivo Imaging of Tumor Hypoxia. *Anal. Chem.* **2011**, *83*, 9039−9046.
(3) Ji, J.; Rosenzweig, N.; Jones, I.; Rosenzweig, Z. Novel Fluorescent Oxygen Indicator for Intracellular Oxygen Measurements. *J. Biomed. Opt.* **2002**, *7*, 404−409.
(4) Lecoq, J.; Parpaleix, A.; Roussakis, E.; Ducros, M.; Houssen, Y. G.; Vinogradov, S. A.; Charpak, S. Simultaneous Two-Photon Imaging of Oxygen and Blood Flow in Deep Cerebral Vessels. *Nat. Med.* **2011**, *17*, 893−898.
(5) Suresh, S.; Srivastava, V. C.; Mishra, I. M. Techniques for Oxygen Transfer Measurement in Bioreactors: A Review. *J. Chem. Technol. Biotechnol.* **2009**, *84*, 1091−1103.
(6) Wang, X.-d.; Wolfbeis, O. S. Optical Methods for Sensing and Imaging Oxygen: Materials, Spectroscopies and Applications. *Chem. Soc. Rev.* **2014**, *43*, 3666−3761.
(7) Wang, X.-d.; Stolwijk, J. A.; Lang, T.; Sperber, M.; Meier, R. J.; Wegener, J.; Wolfbeis, O. S. Ultra-Small, Highly Stable, and Sensitive Dual Nanosensors for Imaging Intracellular Oxygen and pH in Cytosol. *J. Am. Chem. Soc.* **2012**, *134*, 17011−17014.
(8) Habibagahi, A.; Mebarki, Y.; Sultan, Y.; Yap, G. P. A.; Crutchley, R. J. Water-Based Oxygen-Sensor Films. *ACS Appl. Mater. Interfaces* **2009**, *1*, 1785−1792.
(9) Fercher, A.; Borisov, S. M.; Zhdanov, A. V.; Klimant, I.; Papkovsky, D. B. Intracellular O-2 Sensing Probe Based on Cell-

DOI: 10.1021/acsami.5b00403
ACS Appl. Mater. Interfaces 2015, 7, 8606−8614

Penetrating Phosphorescent Nanoparticles. *ACS Nano* **2011**, *5*, 5499−5508.
(10) Thomas, P. C.; Halter, M.; Tona, A.; Raghavan, S. R.; Plant, A. L.; Forry, S. P. A Noninvasive Thin Film Sensor for Monitoring Oxygen Tension During in Vitro Cell Culture. *Anal. Chem.* **2009**, *81*, 9239−9246.
(11) Baleizao, C.; Nagl, S.; Schaeferling, M.; Berberan-Santos, M. N.; Wolfbeis, O. S. Dual Fluorescence Sensor for Trace Oxygen and Temperature with Unmatched Range and Sensitivity. *Anal. Chem.* **2008**, *80*, 6449−6457.
(12) Tian, Y. Q.; Shumway, B. R.; Gao, W. M.; Youngbull, C.; Holl, M. R.; Johnson, R. H.; Meldrum, D. R. Influence of Matrices on Oxygen Sensing of Three Sensing Films with Chemically Conjugated Platinum Porphyrin Probes and Preliminary Application for Monitoring of Oxygen Consumption of Escherichia coli (E. coli). *Sens. Actuators, B* **2010**, *150* (2), 579−587 (Oct. 28).
(13) Xue, R.; Behera, P.; Xu, J.; Viapiano, M. S.; Lannutti, J. J. Polydimethylsiloxane Core−Polycaprolactone Shell Nanofibers as Biocompatible, Real-Time Oxygen Sensors. *Sens. Actuators, B* **2014**, *192*, 697−707.
(14) Wang, L.-Y.; Xu, Y.; Lin, Z.; Zhao, N.; Xu, Y. Electrospinning Fabrication and Oxygen Sensing Properties of Cu(I) Complex−Polystyrene Composite Microfibrous Membranes. *J. Lumin.* **2011**, *131*, 1277−1282.
(15) Quaranta, M.; Borisov, S.; Klimant, I. Indicators for Optical Oxygen Sensors. *Bioanal. Rev.* **2012**, *4*, 115−157.
(16) Tian, Y. Q.; Shumway, B. R.; Meldrum, D. R. A New Cross-Linkable Oxygen Sensor Covalently Bonded into Poly(2-hydroxyethyl methacrylate)-*co*-Polyacrylamide Thin Film for Dissolved Oxygen Sensing. *Chem. Mater.* **2010**, *22*, 2069−2078.
(17) Spellane, P. J.; Gouterman, M.; Antipas, A.; Kim, S.; Liu, Y. C. Porphyrins. 40. Electronic Spectra and Four-orbital Energies of Free-Base, Zinc, Copper, and Palladium Tetrakis(perfluorophenyl)-porphyrins. *Inorg. Chem.* **1980**, *19*, 386−391.
(18) Lai, S.-W.; Hou, Y.-J.; Che, C.-M.; Pang, H.-L.; Wong, K.-Y.; Chang, C. K.; Zhu, N. Electronic Spectroscopy, Photophysical Properties, and Emission Quenching Studies of an Oxidatively Robust Perfluorinated Platinum Porphyrin. *Inorg. Chem.* **2004**, *43*, 3724−3732.
(19) Kneas, K. A.; Demas, J. N.; DeGraff, B. A.; Periasamy, A. Fluorescence Microscopy Study of Heterogeneity in Polymer-Supported Luminescence-Based Oxygen Sensors. *Microsc. Microanal.* **2000**, *6*, 551−562.
(20) Evans, R. C.; Douglas, P. Design and Color Response of Colorimetric Multilumophore Oxygen Sensors. *ACS Appl. Mater. Interfaces* **2009**, *1*, 1023−1030.
(21) McKeen, L. W. *Permeability Properties of Plastics and Elastomers*, 3rd ed.; William Andrew Applied Science: Norwich, NY, USA2012.
(22) Arai, T.; Tanaka, M.; Kawakami, H. Porphyrin-Containing Electrospun Nanofibers: Positional Control of Porphyrin Molecules in Nanofibers and Their Catalytic Application. *ACS Appl. Mater. Interfaces* **2012**, *4*, 5453−5457.
(23) Nam, J.; Huang, Y.; Agarwal, S.; Lannutti, J. Materials Selection and Residual Solvent Retention in Biodegradable Electrospun Fibers. *J. Appl. Polym. Sci.* **2008**, *107*, 1547−1554.
(24) Hartmann, P.; Leiner, M. J. P.; Lippitsch, M. E. Luminescence Quenching Behavior of an Oxygen Sensor-Based on a Ru(II) Complex Dissolved in Polysyrene. *Anal. Chem.* **1995**, *67*, 88−93.
(25) Reneker, D. H.; Yarin, A. L.; Zussman, E.; Xu, H., Electrospinning of Nanofibers from Polymer Solutions and Melts. In *Advances in Applied Mechanics*; Aref, H., van der Giessen, E., Eds.; Elsevier: Amsterdam, 2007; Vol. *41*, pp 43−346.
(26) Xue, R.; Behera, P.; Viapiano, M. S.; Lannutti, J. J. Rapid Response Oxygen-Sensing Nanofibers. *Mater. Sci. Eng., C* **2013**, *33*, 3450−3457.
(27) Lakowicz, J. R. *Principles of Fluorescence Spectroscopy*, 4th ed.; Springer: New York, 2006.
(28) Demas, J. N.; DeGraff, B. A.; Xu, W. Modeling of Luminescence Quenching-Based Sensors: Comparison of Multisite and Nonlinear Gas Solubility Models. *Anal. Chem.* **1995**, *67*, 1377−1380.
(29) Grist, S. M.; Chrostowski, L.; Cheung, K. C. Optical Oxygen Sensors for Applications in Microfluidic Cell Culture. *Sensors* **2010**, *10*, 9286−9316.
(30) Eastwood, D.; Gouterman, M. Porphyrins: XVIII. Luminescence of (Co), (Ni), Pd, Pt Complexes. *J. Mol. Spectrosc.* **1970**, *35*, 359−375.
(31) Borisov, S. M.; Lehner, P.; Klimant, I. Novel Optical Trace Oxygen Sensors Based on Platinum(II) and Palladium(II) Complexes with 5,10,15,20-meso-Tetrakis-(2,3,4,5,6-pentafluorphenyl)-Porphyrin Covalently Immobilized on Silica-Gel Particles. *Anal. Chim. Acta* **2011**, *690*, 108−115.
(32) Kellner, K.; Liebsch, G.; Klimant, I.; Wolfbeis, O. S.; Blunk, T.; Schulz, M. B.; Gopferich, A. Determination of Oxygen Gradients in Engineered Tissue Using a Fluorescent Sensor. *Biotechnol. Bioeng.* **2002**, *80*, 73−83.
(33) Klimant, I.; Wolfbeis, O. S. Oxygen-Sensitive Luminescent Materials Based on Silicone-Soluble Ruthenium Diimine Complexes. *Anal. Chem.* **1995**, *67*, 3160−3166.
(34) Sinkala, E.; Eddington, D. T. Oxygen Sensitive Microwells. *Lab Chip* **2010**, *10*, 3291−3295.
(35) Wang, X.; Peng, H.; Ding, H.; You, F.; Huang, S.; Teng, F.; Dong, B.; Song, H. Biocompatible Fluorescent Core-Shell Nanoparticles for Ratiometric Oxygen Sensing. *J. Mater. Chem.* **2012**, *22*, 16066−16071.
(36) Abdel-Shafi, A. A.; Beer, P. D.; Mortimer, R. J.; Wilkinson, F. Photosensitized Generation of Singlet Oxygen from Vinyl Linked Benzo-Crown-Ether−Bipyridyl Ruthenium(II) Complexes. *J. Phys. Chem. A* **1999**, *104*, 192−202.
(37) Moreno, M. J.; Monson, E.; Reddy, R. G.; Rehemtulla, A.; Ross, B. D.; Philbert, M.; Schneider, R. J.; Kopelman, R. Production of Singlet Oxygen by Ru(dpp(SO3)(2))(3) Incorporated in Polyacrylamide PEBBLES. *Sens. Actuators, B* **2003**, *90*, 82−89.
(38) Rao, S. S.; Nelson, M. T.; Xue, R.; DeJesus, J. K.; Viapiano, M. S.; Lannutti, J. J.; Sarkar, A.; Winter, J. O. Mimicking White Matter Tract Topography Using Core−shell Electrospun Nanofibers to Examine Migration of Malignant Brain Tumors. *Biomaterials* **2013**, *34*, 5181−5190.

DOI: 10.1021/acsami.5b00403
ACS Appl. Mater. Interfaces 2015, 7, 8606−8614